

Simulated Heat Transfer out of a Metallic Cruciform CANDU Fuel Element

L.P. Palumbo*¹¹*McMaster University, 1280 Main Street West, Hamilton, Canada.*

(Dated: 11 January 2018)

Preliminary FlexPDE simulations were run to quantify the temperature distribution and surface heat flux conditions in a theoretical Uranium-Zirconium alloy, helical, cruciform shaped fuel element. A thermohydraulic model of the CANDU-6 pressure tube was created and used to predict a single phase convection heat transfer coefficient of $6.59 \text{ W/cm}^2\text{K}$ for a metal fuel element bundle, a 32% enhancement compared to conventional fuel bundle. At the conventional CANDU fuel pellet centerline melting power level of 70 kW/m , the metal alloy fuel had a simulated peak temperature of 610°C , which is 1115°C below its solidus melting temperature. The heat flow inside the fuel element was not radially symmetrical, and the surface normal to the short axis of the cruciform had the highest heat flux. The simulation indicates the high heat flux regions would produce sustained subcooled nucleate boiling at linear power levels above 40 kW/m .

PACS numbers: 28.41.Fr, 28.41.Bm, 28.41.Ak

Keywords: CANDU, fuel bundle, fuel element, metallic nuclear fuel, U-Zr

I. INTRODUCTION

CANDU-6 is a horizontal pressure tube type commercial nuclear power reactor system. Each of the 380 pressurized tubes in the reactor core contains 12 cylindrical bundles of nuclear fuel elements being actively cooled by forced convection of isotopically enriched heavy water.¹ Each fuel bundle is a 0.5 m long, 10.24 cm diameter, array of 37 hollow tubes 1.308 cm in diameter, with end plates to hold the bundle together. The fuel bundle is made out of a corrosion resistant and relatively neutron transparent alloy known as Zircaloy-4.²

Each fuel element is filled with 19 mm long pellets of the dense Uranium containing ceramic, UO_2 . As the Uranium fissions inside the reactor, the pellets undergo almost uniform volumetric heating. UO_2 has a thermal conductivity of $2\text{-}4 \text{ W/mK}$ in its normal temperature operating range, and as its temperature is increased, its thermal conductivity decreases.³ Because of its low, and inversely temperature dependent thermal conductivity, a fuel pellet can experience a 1500°C temperature differential between its centerline and surface.⁴

The highest pellet centerline temperatures are found in the outer fuel element of a bundle near the axial and azimuthal center of the reactor core at an intermediate burnup of 40 MWh/kgU , these elements have a maximum linear power of 57 kW/m .⁵ The license limit for linear element power is 65 kW/m in a CANDU-6 reactor because high power experiments found fuel pellets begin melting at 70 kW/m .⁶

Commercial entities in the United States are currently developing twisted, non-circular, solid metal nuclear fuel elements for pressurized water reactors⁷ that enhance heat transfer, and have substantially higher thermal conductivity than UO_2 . If adapted to CANDU, a fuel bundle of metal fuel elements may remove the power constraint caused by pellet centerline melting.

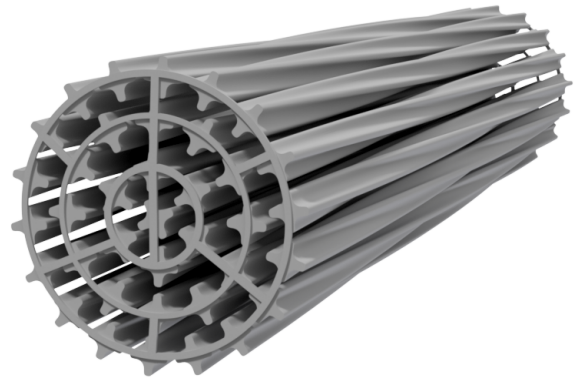


FIG. 1. A CANDU 37 element fuel bundle visualized with helical cruciform fuel elements.

A. Metal Nuclear Fuel

Pure Uranium metal would be an obvious choice for metal fuel due to its high thermal conductivity and maximum nuclear fuel density, however it has a low melting temperature and swells substantially at low burnup levels.⁸ Historically Uranium metal has been alloyed with 10% Zirconium to increase the melting temperature and reduce the burnup swelling, although it is still found to axially swell 8% at 1% atom burnup⁹, an unacceptable amount for a CANDU pressure tube designed to hold bundles of a fixed length.

Irradiation swelling in nuclear fuel is caused by the build up of Xe and Kr fission gas bubbles.⁹ U-Zr alloy with a low Zirconium composition forms the alloy's α -phase crystal structure which is susceptible to swelling.⁸ A U-Zr alloy at 70% Zirconium atom composition has a solidus melting temperature of 1725°C and forms the

δ -phase crystal structure below 616°C ⁸, this structure is resistant to irradiation swelling.⁷ The analysis in this study assumes U-70at%Zr is the fuel alloy.

Cladding metallic nuclear fuel can be achieved by co-extrusion of the fuel inside a layer of cladding⁷, the cladding is assumed to be Zircaloy-4 due to its successful deployment in existing reactors and preexisting supply chain.² Co-extrusion benefits heat transfer by eliminating gap thermal resistance at all temperatures between layers because they are welded together during hot extrusion.

The thermal conductivity of the fuel alloy is modeled by equation 1.¹⁰

$$k_f = -9 \times 10^{-11}T^3 + 4 \times 10^{-7}T^2 - 0.0002T + 0.114 \quad (1)$$

The thermal conductivity of the Zircaloy-4 cladding is given by Equation 2.¹¹

$$k_c = 0.113 + 2.25 \times 10^{-5}T + 0.725 \times 10^{-7}T^2 \quad (2)$$

Where:

T = temperature in K

k = thermal conductivity in W/cmK

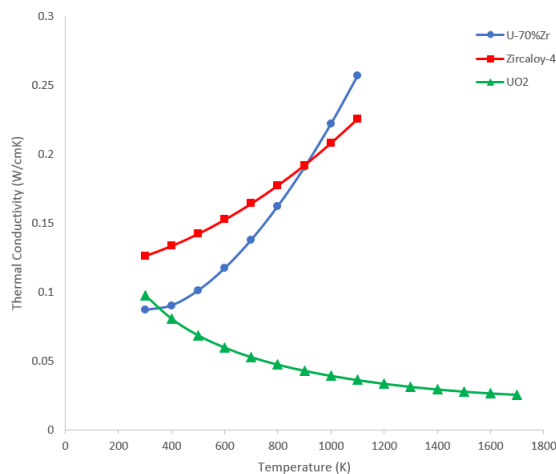


FIG. 2. Thermal Conductivity of traditional UO_2 fuel and Zircaloy-4 cladding compared to the proposed U-70%Zr alloy.

B. Heat Transport Mechanisms

1. Surface Convection

Nuclear heat is transported away from the fuel bundles by pumping 24 Kg/s of D_2O through each pressure tube at an average static pressure of 10.875 MPa(a) and an average temperature of 288°C .¹ This analysis is considering the subcooled liquid flow regime where the primary heat transport phenomenon is one phase, forced convection by highly turbulent flow.¹²

As the wall temperature passes the saturation temperature associated with the coolant's pressure, subcooled

nucleate boiling emerges as a secondary heat transfer mechanism.¹³

Finally, as the wall temperature continues to rise, the localized subcooled boiling forms a layer of bubbles that begins insulating the fuel element surface, this is known as departure from nucleate boiling (DNB)⁴, the heat flux as a function of wall temperature reaches a local maximum at this point before it begins falling towards the Leidenfrost point.¹²

2. Internal Conduction

Inside the fuel element, heat is transported from the fission heated fuel region, through the cladding, to the fuel element wall. Conduction heat transport is dependent on the divergence of the temperature gradient multiplied by the local thermal conductivity. Equation 3 is the time independent heat equation and describes the steady state balance of volumetric thermal power generation in the fuel, s W/cm³, and conduction to its surface.

$$-\nabla \cdot (k\nabla T) + s = 0 \quad (3)$$

C. CANDU Hydraulic Diameter

Conventional, and well documented thermohydraulic relationships for internal turbulent flows can be used for non circular pipes if the equivalent hydraulic diameter is substituted instead.¹⁴ The hydraulic diameter of flow through a fueled CANDU pressure tube is given by Equation 4.¹⁵

$$D_H = \frac{4[\frac{\pi D_{PT}}{4} - 37A_{element}]}{37P_{element} + \pi D_{PT}} \quad (4)$$

II. MODELING APPROACH

A. Hydraulic Modeling

To model the nuclear fuel element's surface thermal boundary condition, the hydraulic conditions need to be calculated and friction factor determined. The pressure drop across 12 conventional CANDU fuel bundles in a 5.94 m fuel channel is 838 kPa¹, and based on private communications with Dr. J. Luxat, the convection coefficient is 5 W/cm²K. In Table II, the friction factor required to yield the specified convection coefficient is listed, and using Equation 5, the apparent geometry dependent minor loss coefficient K is determined and listed in Table I.

$$\Delta p = \frac{fL}{D_H 2} \rho v^2 + \frac{\Sigma K}{2} \rho v^2 \quad (5)$$

In a pressure tube loaded with fuel bundles consisting of 37 cruciform U-Zr metal fuel elements, as shown in Figure 1, the minor loss coefficient is calculated by assuming the front and back of every fuel bundle is a orifice plate, and is listed in Table I. The minor loss is expected to be lower than in a conventional fuel channel due to the larger flow area and lack of need for spacers.

M.M.K. Bhuiya *et al.* found comparing a twisted tape with an array of linear aligned perforations, to a plain tube, showed increases in friction factor at all Reynolds numbers tested.¹⁶ The combination of helically twisting flow, and of flow through aligned holes is assumed analogous to the combination of subchannel linear flow and induced rotational flow across the helical fuel elements encountered in the metal CANDU fuel bundle. The enhancement did however show diminishing improvement as Reynolds number was increased, so an empirical relation was created here to extrapolate the increase in friction factor to higher Reynolds numbers in this analysis.

$$\Delta f = 151.87Re^{-0.817} \quad (6)$$

The enhanced friction factor due to the helical geometry of the metal fuel elements predicted with Equation 6 is listed in Table II.

The larger flow area of the U-Zr metal fuel channel produces a lower pressure drop for any given mass flow rate compared to the conventional fuel channel. The flow rate in the metal fuel bundle channel was modeled as 27.7 kg/s to match the pressure drop of the conventional channel, because the CANDU-6 reference pumping power is constant irrespective of the fuel channel conditions.

TABLE I. The hydraulic parameters of a conventional and metal CANDU fuel channel with equivalent pressure drops.

Fuel	K	D_H (cm)	Re	\dot{M} (kg/s)
UO ₂	15.2	0.743	525000	24.0
U-Zr	12	1.19	972000	27.7

B. Convection Modeling

The single phase convection heat flux out of the fuel element surface is modeled as a function of the temperature difference between the surface and the bulk coolant temperature by Equation 7.

$$q_c'' = h(T_w - T_b) \quad (7)$$

Where h is the convection coefficient evaluated in Equation 8 as a function of the coolants thermal conductivity and the system's dimensionless Nusselt number.¹⁴

$$h = \frac{(Nu)(k)}{D_{H,thermal}} \quad (8)$$

$D_{H,thermal}$ is the hydraulic diameter from Equation 4 with the denominator only considering the heater perimeter not the total wetted perimeter.

The Nusselt number can be calculated using the Gnielinski Equation 9¹⁴, given the Prandtl number of D₂O is 1.046 at 288°C and 10.875 MPa.¹⁷

$$Nu = \frac{(\frac{f}{8})(Re - 1000)Pr}{1 + 12.7(\frac{f}{8})^{0.5}(Pr^{\frac{2}{3}} - 1)} \quad (9)$$

A correction is applied to the Nusselt number for the case of a narrow annulus and an adiabatic outer wall in equation 10.¹⁸

$$\frac{Nu'}{Nu} = 0.86 \left(\frac{D_{PT} - D_H}{D_{PT}} \right)^{-0.16} \quad (10)$$

TABLE II. Convection parameters compared between conventional and the proposed Metal fuel bundles.

Fuel	f	$D_{H,thermal}$ (cm)	Nu	h (W/cm ² K)
UO ₂	0.0157	0.901	918	5.00
U-Zr	0.0176	1.43	1920	6.59

C. Subcooled Boiling Modeling

In the event the surface of the fuel element exceeds the saturation temperature of the bulk coolant, nucleate boiling emerges as a conditional heat transport mechanism. Equation 11 is the Jens-Lottes subcooled boiling heat transfer model, where q_b'' is the surface heat transfer coefficient in units of W/cm²K, and P is the local pressure of the coolant in MPa.

$$q_b'' = (2.56 \times 10^{-4})e^{\frac{P}{1.55}}(T_w - T_b)^4 \quad (11)$$

To model the transition from single phase convection to boiling heat transfer, the larger of the two heat transfer coefficients is used.¹³

$$q'' = \begin{cases} 6.59(T_w - T_b), & \text{otherwise} \\ 0.2853(T_w - T_b)^4, & \text{if } q_b'' > q_c'' \end{cases}$$

III. RESULTS AND DISCUSSION

The steady state heat equation, given in Equation 3, was solved with the conditional surface boundary given in the subcooled boiling modeling section, for a cross section of a metal CANDU fuel element using the multi-physics, finite element simulation package, FlexPDE.

TABLE III. Simulated peak surface and centerline temperatures in high power fuel elements.

Linear Power kW/m	Max T $^{\circ}C$	Max Surface T $^{\circ}C$	Fission Power W/cm^3
27.5	436	306	500
40	495	315	730
57	565	321	1042
65	593	321	1188
70	610	321	1279
75	627	322	1370
80	644	322	1462

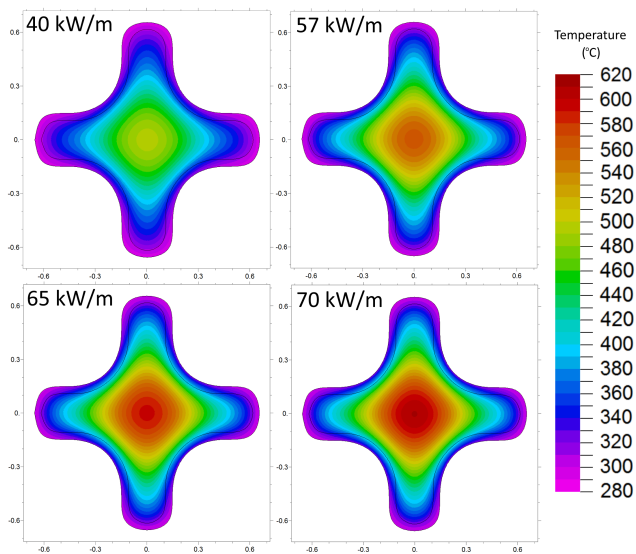


FIG. 3. A comparison of the steady-state temperature distribution in 4 cruciform fuel element cross sections. $57 kW/m$ is the maximum linear power in operating CANDU-6 reactors, $70 kW/m$ would begin melting a conventional fuel element.

The centerline maximum temperatures documented in Table III show the metal CANDU fuel element was over $1000^{\circ}C$ below its solidus melting temperature of $1725^{\circ}C$ ⁸ at all power levels tested, including up to 40% higher than current max operating power levels.

The centerline temperature of the fuel element exceeded the γ -phase transition temperature of $616^{\circ}C$ between linear power levels 70-75 kW/m . At all power levels below the current license limit of 65 kW/m , the metal fuel element is predicted to remain in the desirable δ -phase. If the fuel did transition to the γ -phase of U-Zr, it also has low irradiation swelling properties⁸, however it is unknown if repeated operational cycling between γ and δ -phase crystal structure is undesirable from a thermo-mechanical or nuclear properties perspective.

At a 40 kW/m fuel element power level, surface temperatures over the subcooled nucleate boiling temperature of $315^{\circ}C$ were generated. Figure 4 shows the concen-

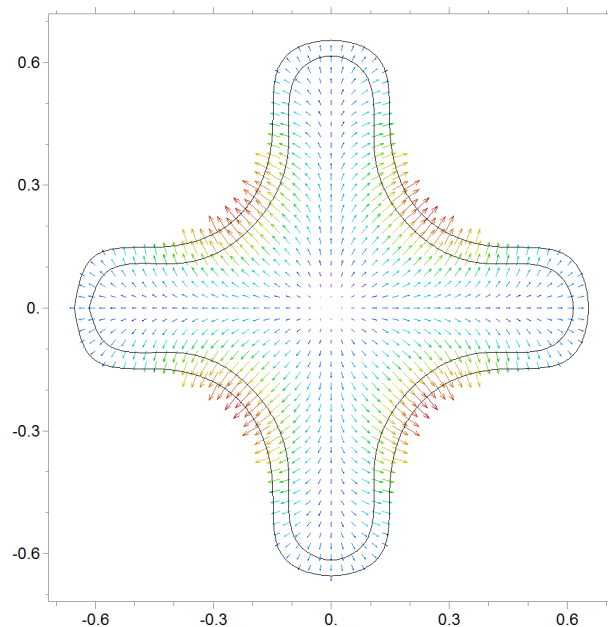


FIG. 4. Spatial heat flow visualized with a vector field plot of temperature gradient vectors generated during a $57 kW/m$ simulation.

trated heat flow along the short axis of the cruciform, this pattern was consistent at all power levels tested. A metal cruciform fuel element operating at, or above, 40 kW/m would produce sustained, localized subcooled boiling. It would not be possible to maintain a near 0% exit steam quality at an average pressure of 10.875 MPa, in high power fuel channels with this fuel design.

As the fuel element fission power increased past 57 kW/m , as seen in Table III, the maximum surface temperature plateaued, and instead the hot region in the indented portion of the cruciform broadened. Due to the non-circular geometry, any transition in heat transfer regime will be spread out over a power dissipation range, this could be a benefit when considering maximum heat flux scenarios where one region of the fuel element may be in dryout or departure from nucleate boiling, and the outer portion of the fin region may still be in a boiling or convection regime.

IV. CONCLUSIONS

Simulation of the heat transport out of a cruciform Uranium-Zirconium CANDU fuel element suggest centerline fuel melting onset at 70 kW/m linear power would not be a limiting factor as it is in conventional UO_2 ceramic fuel elements. Furthermore fuel elements simulated at the maximum operating element power of 57 kW/m demonstrated $>1000^{\circ}C$ thermal margins to melting.

The cruciform geometry increases heat transfer area and depresses maximum temperature, however the Flex-PDE simulation showed focused heat flow to the indented

portions of the cruciform, and these regions would produce sustained boiling at element power levels found in a CANDU-6 nuclear fuel channel.

Many considerations would go into selecting metal CANDU fuel, including enrichment requirements, reactivity implications based on different fuel absorption and scattering cross sections, lower resonance absorption due to lower average temperatures, changes in burnup dynamics due to the change in ^{235}U fission versus ^{239}Pu breeding ratios, and primary heat transport system steam quality limits. From a thermohydraulic perspective, this analysis suggest development of cruciform Uranium-Zirconium fuel elements could lead to increased thermal margins or an up-rate of existing CANDU reactor's power output.

ACKNOWLEDGMENTS

The author would like to thank Dr. Turak and K. Groves for their feedback and guidance throughout the research and writing of this paper, Dr. Minnick for his enthusiastic and expert help with FlexPDE and heat transfer physics, and Dr. J. Luxat for his excellent course material and CANDU technical data.

Notes and References

*Author to whom correspondence should be addressed.
Electronic mail: lpalumbo@vistaengineering.com

- ¹CANDU 6 Technical Summary. Atomic Energy Canada Ltd., 2005.
- ²R.D. Page. *Canadian Power Reactor Fuel*. Atomic Energy Canada Ltd.
- ³J.H. Harding and D.G. Martin. A recommendation for the thermal conductivity of uo2. *Journal of Nuclear Materials*, 166(3): 223 – 226, 1989.
- ⁴A Harms. *An Introduction to the CANDU Nuclear Energy Conversion System*. McMaster University, 1972. Retrieved from: <https://canteach.candu.org/Content>
- ⁵A Manzer. Candu fuel performance. Technical report, Atomic Energy Canada Ltd., Mississauga, Ontario, Canada, 1996.
- ⁶Song Wenhui and A Manzer. Candu fuel performance. *AECL, Shanghai Nuclear Design and Research Institute*.
- ⁷A Totemeier, N Shaprio, and S Vaidyanathan. Lightbridge corporation's advanced metallic fuel.
- ⁸Marcio Soares Dias and Joao Roberto L de Mattos. Uranium-zirconium based alloys part i: reference points for thermophysical properties.
- ⁹Gerard L. Hofman, R. G. Pahl, C. E. Lahm, and D. L. Porter. Swelling behavior of u-pu-zr fuel. *Metallurgical Transactions A*, 21(2):517–528, Feb 1990.
- ¹⁰Yeon Soo Kim, Tae Won Cho, and Dong-Seong Sohn. Thermal conductivities of actinides (u, pu, np, cm, am) and uranium-alloys (uzr, upuzr and uputuzr). *Journal of Nuclear Materials*, 445(1):272 – 280, 2014.
- ¹¹Masayuki MURABAYASHI, Shigenori TANAKA, and Yoichi TAKAHASHI. Thermal conductivity and heat capacity of zircaloy-2, -4 and unalloyed zirconium. *Journal of Nuclear Science and Technology*, 12(10):661–662, 1975.
- ¹²J.C. Luxat. Two-phase flow: Flow regimes, pressure drop, boiling heat transfer, and critical heat flux. McMaster Engineering Physics 4NE3 Lecture Notes, .
- ¹³Boris Lekakh, Mujid S Kazimi, and John E Meyer. Boiling heat transfer for high velocity flow of highly subcooled water. Technical report, Dept. of Nuclear Engineering, Massachusetts Institute of Technology, 1999.
- ¹⁴Yunus A Cengel, John M Cimbala, and Robert H Turner. *Fundamentals of thermal-fluid sciences*. McGraw-Hill, 2012.
- ¹⁵J.C. Luxat. Nuclear heat transport: Single phase flow and heat transfer. McMaster Engineering Physics 4NE3 Lecture Notes, .
- ¹⁶M.M.K. Bhuiya, M.S.U. Chowdhury, M. Saha, and M.T. Islam. Heat transfer and friction factor characteristics in turbulent flow through a tube fitted with perforated twisted tape inserts. *International Communications in Heat and Mass Transfer*, 46 (Supplement C):49 – 57, 2013.
- ¹⁷N. Matsunaga and A. Nagashima. Transport properties of liquid and gaseous d2o over a wide range of temperature and pressure. *Journal of Physical and Chemical Reference Data*, 12(4):933–966, 1983.
- ¹⁸B.S. Petukhov and L.I. Roizen. General dependences for heat treatment at turbulent fluid flow in an annulus. *Izvestiya of the USSR Academy of Sciences. Energy and transport*, (1):103, 1967.